Metabolism Clinical and Experimental 91 (2019) 18–29

Contents lists available at ScienceDirect

Metabolism Clinical and Experimental

journal homepage: www.metabolismjournal.com

Metabolomics profiling of metformin-mediated metabolic reprogramming bypassing AMPKα☆

Min Yan [a,b,1], Huan Qi [a,1], Tian Xia [a], Xinjie Zhao [a], Wen Wang [a,b], Zhichao Wang [a,b], Chang Lu [a,c], Zhen Ning [a,c], Huan Chen [a,b], Tongming Li [a], Dinesh Singh Tekcham [a], Xiumei Liu [a], Jing Liu [a], Di Chen [a], Xiaolong Liu [a], Guowang Xu [a,*], Hai-long Piao [a,b,*]

[a] CAS Key Laboratory of Separation Science for Analytical Chemistry, Scientific Research Center for Translational Medicine, Dalian Institute of Chemical Physics, Chinese Academy of Sciences, Dalian 116023, China
[b] University of Chinese Academy of Sciences, Beijing 100049, China
[c] Department of Hepatobiliary Surgery, The First Affiliated Hospital of Dalian Medical University, China

ARTICLE INFO

Article history:
Received 31 August 2018
Accepted 15 November 2018

Keywords:
Metformin
Ampk
Metabolomics
Metabolic flux
Independence

ABSTRACT

Background: Metformin is a first-line drug for treating type 2 diabetes and has gained considerable interest as a potential anticancer agent. Increasing evidence suggests that metformin antagonizes diabetes and tumors through disrupting metabolic homeostasis and altering energy state. However, whether AMP activated protein kinase (AMPK) contributes to such effects of metformin remains controversial.

Methods: We performed integrative metabolomics analyses to systematically examine the effects of metformin on metabolic pathways in *Prkaa1* wild type (WT) and knock-out (KO) mouse embryonic fibroblast (MEF) cells as well as human cells based on gas chromatography–mass spectrometry and capillary electrophoresis–mass spectrometry (CE–MS).

Results: Metformin treatment induced metabolic reprogramming and reduced the energy state of both *Prkaa1* WT and KO MEF cells, as evidenced by suppressed tricarboxylic acid (TCA) cycle, elevated lactate production as well as decreased NAD^+/NADH ratio. Additionally, metabolic flux analysis also showed that metformin Ampkα-independently increased metabolic flux from glucose to lactate and decreased metabolic flux from acetyl-CoA to TCA cycle as well as from pyruvate to malate. Moreover, metformin Ampkα-dependently upregulated P-Acc but Ampkα-independently inhibited the levels of P-mTor, P-S6, Lc3, Atgl and P-Erk in MEF cells. Similarly, we demonstrated that a commonly used AMPK agonist 5-Aminoimidazole-4-carboxamide ribonucleotide (AICAR) and fetal bovine serum (FBS) starvation, as a common model for energy stress, both led to Ampkα-independent metabolism alterations in MEF cells. Furthermore, these effects of metformin were also confirmed in human hepatocellular carcinoma (HCC) cells as well as in MCF10A shControl and shPRKAA1 cells. Importantly, we found that metformin could obviously inhibit colony conformation of HCC cells in an Ampkα-independent manner.

Conclusions: Our data highlight a comprehensive view of metabolic reprogramming mediated by metformin as well as AICAR. These observations suggest that metformin could affect cellular metabolism largely bypassing Ampkα, and may provide a new insight for its clinical usage.

Abbreviations: AMPK/Ampk, AMP activated protein kinase; WT, wild type; KO, knock-out; MEF, mouse embryonic fibroblast; GC–MS, gas chromatography–mass spectrometry; CE–MS, capillary electrophoresis–mass spectrometry; TCA, tricarboxylic acid; AICAR, 5-Aminoimidazole-4-carboxamide ribonucleotide; HCC, hepatocellular carcinoma; FBS, fetal bovine serum; T2D, type 2 diabetes; ETC, electron transport chain; HPLC, high performance liquid chromatography; MSTFA, *N*-methyl-*N*-(trimethylsilyl)-trifluoroacetamide; ISS, internal standard solution; P/S, penicillin-streptomycin; TOF, time of flight; HMT, Human Metabolome Technologies; EGF, epidermal growth factor; EP, Eppendorf; QC, quality control; LDS, lithium dodecyl sulfate; PVDF, polyvinylidene fluoride; SD, standard deviation; PCA, principal component analysis; α-KG, α-ketoglutarate; PRPP, 5-Phosphoribosyl 1-pyrophosphate; MID, mass isotopologue distribution.

☆ Dedicated to the 70th anniversary of Dalian Institute of Chemical Physics, CAS

* Corresponding authors at: CAS Key Laboratory of Separation Science for Analytical Chemistry, Dalian Institute of Chemical Physics, CAS, 457 Zhongshan Road, Dalian 116023, China.
E-mail addresses: xugw@dicp.ac.cn (G. Xu), hpiao@dicp.ac.cn (H. Piao).

[1] These authors contributed equally to this work.

https://doi.org/10.1016/j.metabol.2018.11.010
0026-0495/

1. Introduction

Metformin is widely used as a hypoglycemic drug due to its desirable safety and surprising therapeutic efficacy for type 2 diabetes (T2D) [1]. Recently, metformin has been linked to reduced incidence of cancer among diabetics who take this medicine [2–4]. Thus, metformin has gained considerable attention as a potential anticancer agent. Moreover, metformin has also been reported to increase lifespan [5,6] and improve gut flora [7]. However, the precise mechanism of metformin in the treatment of these diseases remains controversial. One of the most possible mechanisms of action is disrupting mitochondrial function, thereby resulting in the alterations to the tricarboxylic acid (TCA) cycle, electron transport chain (ETC) as well as ATP production. Liu et al. revealed that metformin could target the mitochondrial metabolism in ovarian cancer based on an integrative metabolomics analysis [8]. It has also been reported that metformin can suppress cancer cell growth via inhibiting mitochondrial-dependent biosynthesis [9].

AMP-activated protein kinase (AMPK), a heterotrimeric complex composed of α, β and γ subunits, plays a critical role in many biological processes, including metabolism [10,11], cell growth [12], autophagy [13] and apoptosis [14]. As an important cellular energy sensor, AMPK is highly sensitive to the ratios of AMP/ATP and ADP/ATP. Thus, under energy stress, AMPK can be phosphorylated at Thr-172 of α-subunit, then activates a serial of downstream metabolic enzymes to promote ATP generation [15]. Abnormally activated or inhibited AMPK is associated with the pathogenesis of T2D and cancers, which is therefore considered as a potential target for treating these disorders [16,17]. It has been widely accepted that metformin functions as an indirect AMPK agonist [9]. However, whether AMPK as the target of metformin can entirely explain its therapeutic effects still remains controversial. Some studies reveal that the anti-cancer and anti-hyperglycemic effects of metformin have a close link with AMPK activation. For instance, it has been demonstrated that metformin regulated blood sugar through a gut–brain–liver axis by activating duodenal AMPK [18]. Additionally, metformin has also been reported to inhibit tumor growth of non-small cell lung cancer and enhance the sensitivity to ionizing radiation through an ATP-AMPK-dependent pathway [19]. On the contrary, other studies support the notion that AMPK activation is not involved in the mechanism of action of metformin. Isaam et al. reported that metformin induced cell cycle arrest and mTOR inhibition via REDD1 in an AMPK-independent way [20]. Consistently, metformin has also been found to suppress hepatic gluconeogenesis through the reduction of energy state bypassing the LKB1-AMPK signaling pathway [21]. Nevertheless, although numerous researches have focused on the contribution of AMPK to the mechanism of action of metformin, AMPK dependence of metformin on cellular metabolism is still unclear.

To define the AMPK dependence of metformin and understand its mechanism, we carried out integrative metabolomics analyses and metabolic flux assay in *Prkaa1* wild type (WT) and knock-out (KO) mouse embryonic fibroblast (MEF) cells to systematically examine the effect of metformin on metabolic pathways and its correlation with Ampkα. Furthermore, we validated the AMPKα dependence in metformin-treated human hepatocellular carcinoma (HCC) cell lines as well as MCF10A shControl and shPRKAA1 cell lines.

2. Materials and Methods

2.1. Chemicals and Reagents

The detailed information of chemicals and reagents is listed in Supplemental materials.

2.2. Cell Culture and Drug Treatment

Prkaa1 WT and KO MEF cells were a kind gift from Prof. Sheng-Cai Lin in Xiamen University, China [22,23]. Human HCC cell lines (SMMC-7721, BEL-7402, MHCC97H and HCCLM3) were purchased from the National Infrastructure of Cell Line Resource (NSTI, Beijing, China). SNU-449 was purchased form American Type Culture Collection (Manassas, USA). MCF10A shPRKAA1 and shControl cells were sent as a kind gift from Prof. Zhi-Xiong Xiao in Sichuan University, China. The detail information of shRNA used in MCF10A cells was described as previously [24]. MHCC97H shPRKAA1 and shControl cells were also constructed by these shRNA following puromycin screening. The detailed information of cell culture is described in Supplemental materials.

Metformin was dissolved in DMEM or DMEM/F12 (1:1) medium with 100 mM as stock solution. For GC–MS metabolomics and western blotting analyses, MEF and HCC cells were treated with indicated concentrations of metformin (1 or 10 mM) or AICAR (2 mM) and MCF10A cells were treated with 20 mM metformin for 24 h. For CE–MS metabolomics analysis, MEF cells were treated with 10 mM metformin or 0.5 mM AICAR for 24 h. For cell growth assay, cells were treated with metformin (1 or 10 mM) or AICAR (2 mM) for the indicated periods. For metabolic flux analysis, MEF cells were cultured in DMEM medium with 4.5 g/L U-$13C_6$-glucose, 10% dialyzed serum (GEMINI, West Sacramento, USA) and 1% penicillin-streptomycin for 24 h with 10 mM metformin treatment.

2.3. Sample Preparation

For gas chromatography–mass spectrometry (GC–MS) analysis, metabolites were extracted by methanol/water (4:1, v/v, containing 10 μg/mL tridecanoic acid as internal standard). For capillary electrophoresis–mass spectrometry (CE–MS) analysis, metabolites were extracted by 1 mL methanol (containing 200-fold diluted ISS1), 1 mL chloroform, followed by adding 400 μL ultrapure water. The detailed procedures for metabolite extraction are provided in Supplemental materials.

2.4. Metabolomics Analyses

GC–MS based full-scan metabolomics analysis was performed by using GCMS-QP 2010 analytical system (Shimadzu, Japan) as previously described [25]. DB-5 MS capillary column (30 m × 250 μm × 0.25 μm, J&W Scientific, Folsom, CA, USA) was used for sample separation. EI source with 70 eV electron impact was used as ionization mode.

CE–MS based metabolomics and metabolic flux analysis were conducted on CE (G7100A, Agilent, Santa Clara, CA, USA) couple to time of flight (TOF) mass spectrometry (G6224A, Agilent). The fused silica capillary (50 μm i.d. × 80 cm, Human Metabolome Technologies (HMT), Tsuruoka, Japan) was used for sample separation. The pre-analyzed metabolite standard library was used for metabolite qualitative and qualitative (HMT). The analytical methods were used as previously described [26].

2.5. Cell Viability and Proliferation Assay

The detailed protocols of cell viability and proliferation assay are described in Supplemental materials.

2.6. Western Blotting

RIPA buffer was used for cell lysis. Equal amounts of protein were separated by SDS-polyacrylamide gel electrophoresis and transferred to polyvinylidene fluoride (PVDF) membranes (Bio-Rad, Hercules, CA, USA). After primary antibodies incubating overnight at 4 °C, membranes were incubated with HRP-conjugated secondary antibodies at room temperature. The protein bands were visualized by incubated with chemiluminescence (Thermo Fisher Scientific). The detailed procedures and primary antibodies used in this study are described in Supplemental materials.

2.7. Colony Formation Assay

The detailed procedures of two and three-dimensional colony formation assay are provided in Supplemental materials.

2.8. Data Processing and Statistical Analysis

In GC–MS based metabolomics analysis, the metabolite identification and quantification were conducted by ChromaTOF software (LECO, St. Joseph, MI, USA) and GCMS solution software (Shimadzu), respectively. For each sample, the peak area of each metabolite was first normalized to the dry weight of cell protein followed by normalization to the peak area of internal standard. In CE–MS based metabolomics analysis, data analysis was performed by Agilent Qualitative and Quantitative analysis software (Agilent). For each sample, the peak area of each metabolite was normalized to the total peak areas of all metabolites. In metabolic flux analysis, the data were processed by in-lab software SIAM Analyzer to correct natural isotopes and calculate mass isotopologue distribution (MID).

All data were expressed as mean ± standard deviation (SD). Data analyses were carried out by GraphPad software 5.0 (GraphPad Software, USA) and Excel 2010 (Microsoft). Significance was analyzed by using one-way ANOVA followed by Tukey's multiple comparison test for multiple groups and student's *t*-tests for two groups and $p < 0.05$ indicated significant. Principal component analysis (PCA) and heatmap analyses were performed by SIMCA-P software (Umetrics, Umea, Sweden, version 11.0) and Multi Experiment Viewer software (MeV, version 4.8.1), respectively. Pathway analysis was conducted by using on-line software MetaboAnalyst 3.0 [27].

3. Results

3.1. Metabolomics Profiling of Prkaa1 WT and KO MEF Cells

In this study, we systematically investigated the effect of metformin on metabolism by metabolomics profiling. The flow chart of this study is presented in Fig. S1. We first measured the expression of Ampkα in *Prkaa1* WT and KO MEF cells. Compared with WT MEF cells, the levels of Ampkα, P-Ampk and P-Acc were almost absent in KO MEF cells (Fig. 1A). Subsequently, we compared the cell proliferation rate and performed metabolomics profiling between WT and KO MEF cells. As shown in Fig. S2A, WT and KO MEF cells displayed the similar growth rates. Based on GC–MS untargeted metabolomics profiling, we found that there were 44 differential metabolites between these two cells lines (Fig. 1B). Following analysis by online software MetaboAnalyst 3.0, two most obviously altered metabolic pathways were alanine, aspartate and glutamate metabolism as well as tricarboxylic acid (TCA) cycle (Fig. S2B). Of note, TCA intermediates, such as citrate, fumarate and malate, coupled to energy state, were markedly increased in KO MEF cells relative to WT MEF cells (Fig. 1C). Consistent with the previous study [28], lactate production was significantly elevated in KO MEF cells compared with WT MEF cells (Fig. 1D). Additionally, the level of intracellular glucose in KO MEF cells showed a reduction, suggesting an elevation in glucose consumption (Fig. 1E). These results showed a close link between Ampkα and energy metabolism.

3.2. Metformin Affected the Majority of Metabolic Pathways in an Ampkα-independent Manner

Metformin has been reported as an indirect activator of AMPK [29]. We first examined the effect of metformin on Ampkα Thr-172 phosphorylation in WT and KO MEF cells via immunoblot. Following treatment with metformin (10 mM), Ampkα phosphorylation at Thr-172 was remarkably induced in WT MEF cells, whereas it was almost absent in KO MEF cells, as was Ampkα expression (Fig. 2A). Then, we determined the expression of Ampkα downstream proteins, including Acc1, P-Acc, S6, P-S6, mTor, P-mTor, Atgl, Lc3, Erk and P-Erk in WT and KO MEF cells following metformin treatment (Fig. 2A). As expected, P-S6, P-mTor and P-Erk were inactivated by metformin in both WT and KO MEF cells, whereas P-Acc was upregulated only in WT MEF cells. Moreover, metformin remarkably downregulated the levels of Lc3 and Atgl in both WT and KO MEF cells (Fig. 2A).

AMPK has been considered to function as a negative modulator of cell proliferation [30]. Hence, we examined the cell proliferation by using crystal violet staining following 24 h of metformin treatment. Interestingly, metformin exhibited similar anti-proliferative effects on these two cell lines (Fig. 2B, C). These results revealed that the anti-proliferative effects of metformin on MEF cells were largely Ampkα-independent.

Accumulating evidence indicates that the therapeutic effects of metformin against diabetes as well as cancers have been linked to altered metabolic pathways. Thus, we systematically assessed the metabolomics profiling of WT and KO MEF cells using GC–MS and CE–MS analyses following culture with metformin. PCA score plot showed that the MEF cells with different treatments were completely separated (Fig. S3A). Compared with untreated cells, there were totally 62 differential metabolites found out in metformin-treated WT MEF cells and 58 differential metabolites in metformin-treated KO MEF cells, of which 48 metabolites were in the intersection (Fig. S3B). Based on metabolic pathway analysis, we found that aerobic glycolysis, TCA cycle and amino acid metabolism exhibited marked alterations following metformin treatment. We next evaluated the Ampkα dependence of the changes in metabolic pathways observed in Figs. 2D and S4. Notably, metformin significantly decreased the levels of citrate and succinate, the main intermediates during TCA cycle, in both WT and KO MEF cells. Besides, cellular lactate levels, the final product of aerobic glycolysis, were obviously elevated after treatment with metformin regardless of Ampkα. Moreover, metformin also affected majority of amino acids in an Ampkα-independent manner, for example, serine, hypotaurine and 3-methyl-2-oxovaleric acid were upregulated, whereas proline, 4-guanidinobutyric acid and aspartate were downregulated. However, the minority of amino acids showed an Ampkα-dependent alteration, such as phenylalanine, methionine and threonine.

To further understand these alterations, we analyzed the associations among these metabolic pathways by comparing the critical metabolite ratios. As expected, metformin treatment led to a significant reduction in the ratio of citrate/pyruvate and an obvious elevation in the ratio of lactate/pyruvate in both WT and KO MEF cells (Fig. 3A, B). These results indicated that metformin inhibited the entry of pyruvate into the TCA cycle and promoted lactate production bypassing Ampkα. In addition, we observed a marked increase in α-ketoglutarate (α-KG) under metformin treatment. This might result from the contribution of glutamine, which is another source entry into the TCA cycle via generating α-KG by deamination and transamination reactions [9]. Of note, the ratio of α-KG/glutamine was significantly elevated following metformin treatment of WT and KO MEF cells (Fig. 3C). Interestingly, co-culture with glutamine or sodium pyruvate could both reverse metformin-induced growth inhibition (Fig. 3D, E).

Given the high sensitivity of Ampkα in response to the ratio of AMP/ATP or ADP/ATP, we performed CE–MS based metabolomics analysis to figure out the Ampkα dependence of the alterations in nucleotides. As expected, there were significant differences of nucleotide ratios in Ampkα WT and KO MEF cells. Following metformin treatment, WT and KO cells displayed the similar trends in alterations of these nucleotide ratios compared to their untreated cells, although the KO cells showed lower energy state than WT cells (Fig. 4A). Consistently, based on the formula (ATP + 0.5 × ADP) / (ATP + ADP + AMP) [31], the cell energy state was also obviously suppressed by metformin treatment in both WT and KO MEF cells (Fig. 4B). Moreover, metformin treatment reduced the NAD^+/NADH ratio due to NADH accumulation in both two cell lines (Fig. 4C). These findings indicated that metformin could repress the energy generation largely in an Ampkα-independent manner.

3.3. AICAR Induced Remark Metabolic Alterations in an Ampkα-independent Manner

AICAR, an AMP mimic, commonly functions as an AMPK agonist in the laboratory and has also been explored as an anticancer agent [32].

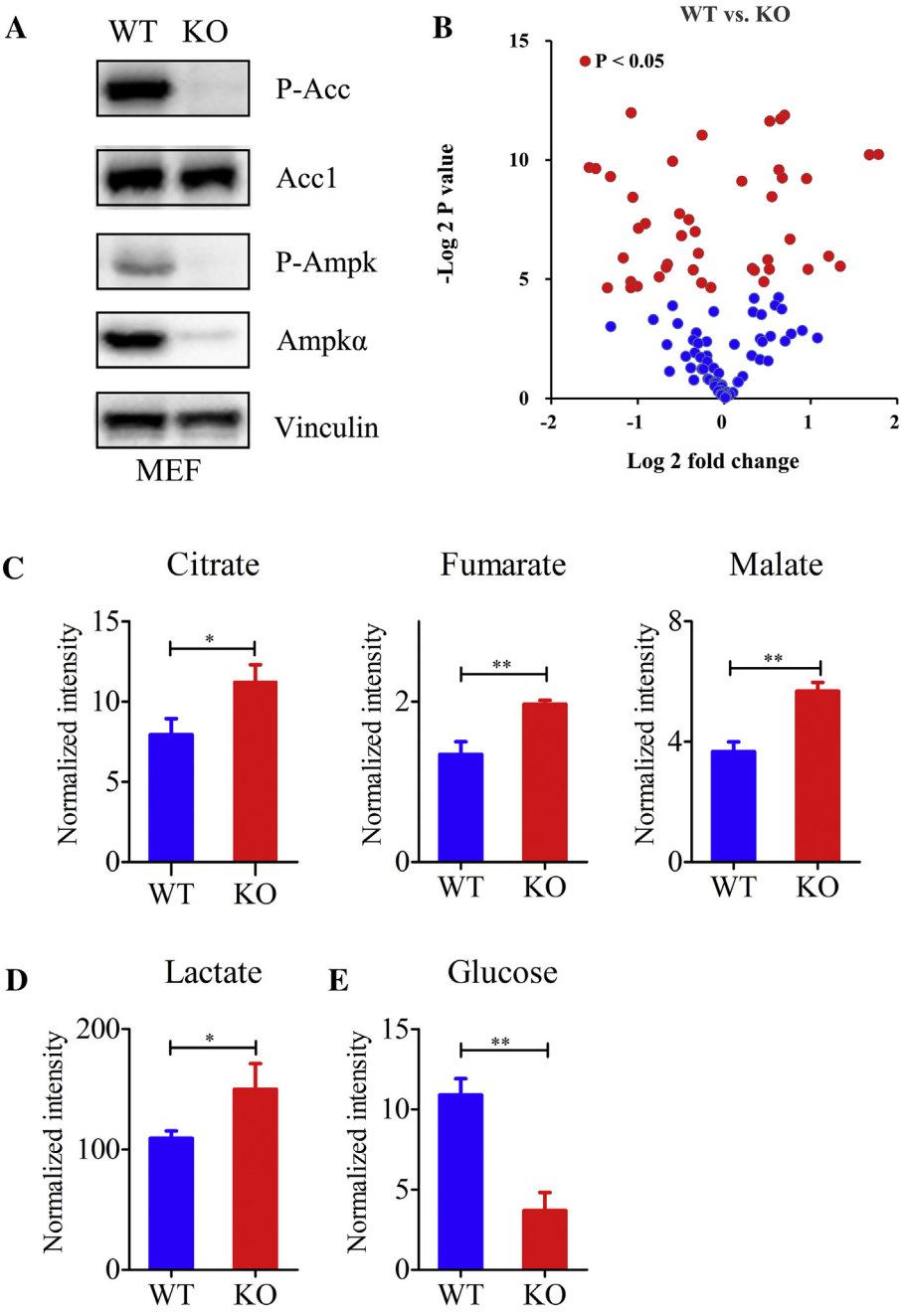

Fig. 1. *Prkaa1* knock-out (KO) MEF cells displayed altered metabolomics profiling compared to *Prkaa1* wild type (WT) MEF cells based on GC–MS. (A) Immunoblot of Ampkα, P-Ampk (T172), Acc1 and P-Acc (S79) in *Prkaa1* WT and KO MEF cells. Vinculin was used as a loading control. (B) Volcano plot of 44 different metabolites between WT and KO MEF cells (n = 3, $p < 0.05$ vs. WT MEF cells). X axis, $\log_2$ (ratio of KO to WT), Y axis, $-\log_2$ (p value). (C–E) The levels of citrate, fumarate, malate, lactate and glucose in WT and KO MEF cells were compared (n = 3). Data are expressed as mean ± SD. Differences between two groups were analyzed by Student t-test. $^{*}p < 0.05$ and $^{**}p < 0.01$ vs. WT MEF cells.

Here, similar to metformin, we also performed a systematically metabolomics screen in order to pinpoint the correlation between AICAR-induced metabolic alterations and Ampkα dependence. We first found that AICAR only activated the Ampkα of WT MEF cells, however, displayed an obviously suppressive effect on the proliferation of both WT and KO MEF cells (Fig. 2A–C), which was in line with the previous observations [28]. In line with metformin, AICAR also upregulated P-Acc only in WT MEF cells but downregulated P-S6, P-mTor, Atgl and P-Erk in both WT and KO MEF cells (Fig. 2A). However, AICAR obviously increased the level of Lc3 in both WT and KO MEF cells, which was in contrast to metformin (Fig. 2A).

Based on GC–MS analysis, we observed 50 differential metabolites in AICAR-treated WT MEF cells and 64 differential metabolites in AICAR-treated KO MEF cells when compared with the untreated cells, of which 44 metabolites were the same (Fig. S3B). Of note, the intracellular glucose levels of both WT and KO MEF cells were dramatically elevated by AICAR treatment, suggesting an Ampkα-independent decrease in glucose consumption (Fig. S4). In contrast to metformin, AICAR caused a remarkable reduction in the lactate level regardless of Ampkα (Fig. S4). Moreover, although citrate and the ratio of citrate/pyruvate had little alteration following AICAR treatment, other TCA intermediates, including α-KG, succinate, fumarate and malate, were all markedly downregulated in both WT and KO MEF cells (Fig. S4). These findings revealed that AICAR treatment could inhibit aerobic glycolysis and the TCA cycle in MEF cells. Importantly, such suppression of AICAR exerted no correlation with Ampkα activity. Additionally, AICAR had little effect on amino acid metabolisms except for several individual amino acids.

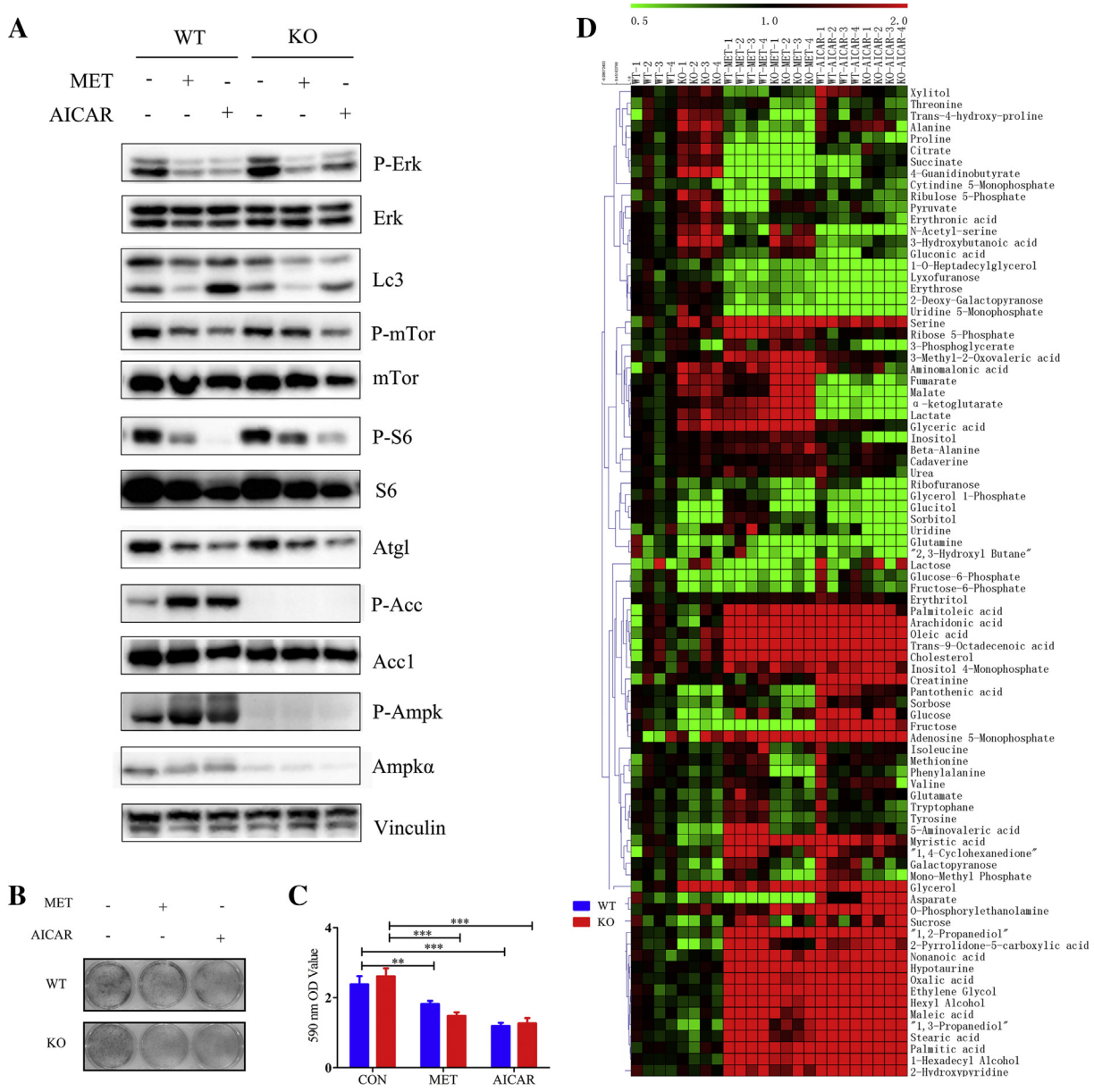

Fig. 2. Metformin and AICAR affected metabolism of MEF cells in an Ampkα-independent manner. (A) The effects of metformin (10 mM) and AICAR (2 mM) on Ampkα, P-Ampk (T172), Acc1, P-Acc (S79), S6, P-S6 (S235/236), mTor, P-mTor (S2448), Lc3, Atgl, Erk and p-Erk (Thr202/Tyr204) expression in WT and KO MEF cells following 24 h of treatment. Vinculin was used as an internal control. (B, C) Cells were stained with 0.1% crystal violet after 24 h of treatments with metformin and AICAR, representative images are shown (B) and cell viability was quantified by extracting with 10% acetic acid and determining at 590 nm (C) (n = 4). (D) Heatmap of main metabolites in WT and KO MEF cells following treatment with metformin (10 mM) and AICAR (2 mM) based on GC–MS. For each metabolite, the average value of untreated WT MEF cells was used for normalization (n = 4). Data are expressed as mean ± SD, $^{**}p < 0.01$ and $^{***}p < 0.001$ vs. the control group. CON indicates control and MET indicates metformin.

Given AICAR-mediated AMPKα activation due to the binding of its metabolic product ZMP to the γ-subunit of AMPK [33], we further investigated the effects of AICAR on nucleotides metabolism in WT and KO MEF cells using CE–MS. As expected, AICAR seriously disrupted the balance of nucleotide metabolisms, as evidenced by a dramatic upregulation in purine metabolites (i.e., ATP, ADP, AMP, GTP, GDP and GMP) and a marked downregulation in pyrimidine metabolites (i.e., CTP, CDP, CMP, UTP, UDP and UMP) (Fig. S5). Furthermore, the level of 5-Phosphoribosyl 1-pyrophosphate (PRPP) was completely suppressed following AICAR treatment, which could be explained by the feedback inhibition of increased purine metabolites. It has been considered that PRPP functions as a critical substrate for UMP synthase catalyzing the conversion of orotate to UMP [34]. In line with such data were the observed accumulation in orotate and reduction in UMP as well as the downstream pyrimidine metabolites. This result is consistent with the previous studies in AICAR-treated multiple myeloma cells [35]. More interestingly, our findings showed that such effects of AICAR on nucleotide metabolisms were independent of Ampkα in MEF cells.

3.4. Metformin Ampkα-independently Promoted Lactate Production and Inhibited TCA Cycle by Metabolic Flux Analysis

To further validate metformin-mediated metabolic alterations, we performed metabolic flux analysis in *Prkaa1* WT and KO MEF cells following metformin treatment. As shown in Fig. 5, the proportion of lactate (M + 0) was decreased and that of lactate (M + 3) was increased following metformin treatment in both *Prkaa1* WT and KO MEF cells, suggesting that metformin led to an Ampkα-independent promotion of lactate production. In addition, TCA cycle intermediates citrate (M + 0), fumarate (M + 0), malate (M + 0), α-KG (M + 0) and succinate (M + 0) were Ampkα-

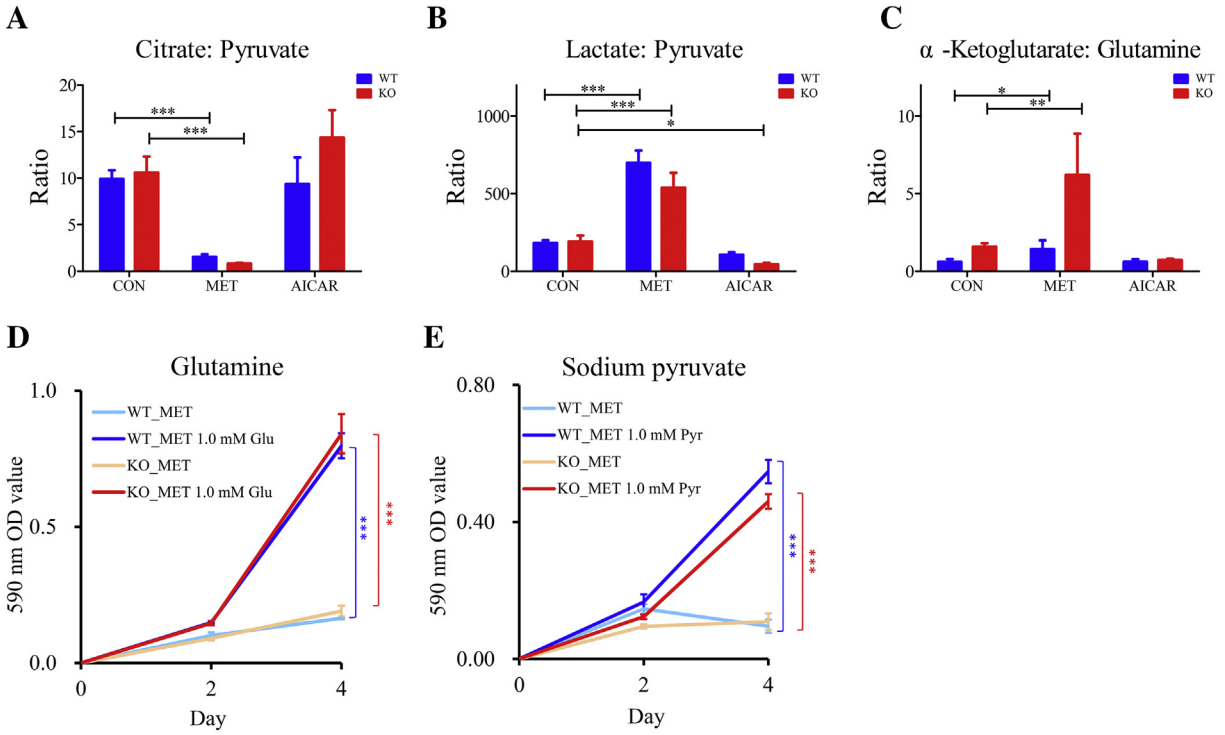

Fig. 3. Glutamine and sodium pyruvate reversed metformin-induced cell growth inhibition. (A–C) Metabolite ratios in MEF cells treated with metformin and AICAR including citrate/pyruvate, lactate/pyruvate and α-ketoglutarate/glutamine were calculated (n = 4). $^{*}p < 0.05$, $^{**}p < 0.01$ and $^{***}p < 0.001$ vs. the control group. (D, E) The effects of glutamine (1 mM, D, n = 3) and sodium pyruvate (1 mM, E, n = 3) on cell viability of 10 mM metformin-treated MEF cells were determined by crystal violet staining. Data are expressed as mean ± SD. $^{***}p < 0.001$ vs. the metformin-treated group. Glu indicates glutamine, and Pyr indicates sodium pyruvate.

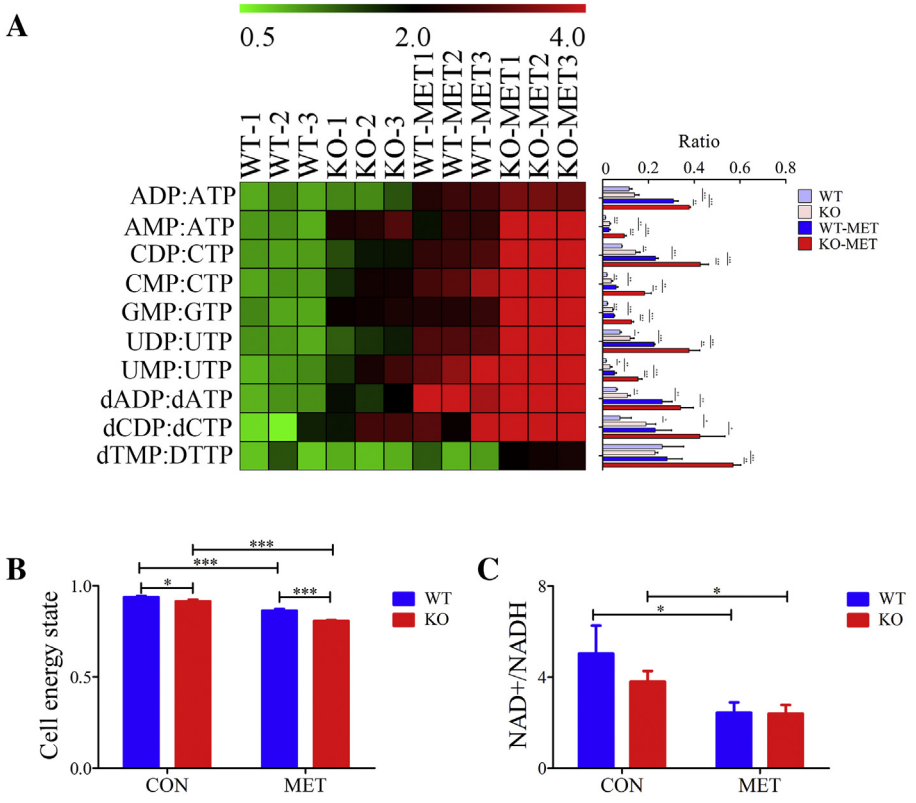

Fig. 4. Metformin significantly reduced cellular energy states in an Ampkα-independent manner. (A) The effect of metformin on nucleotide ratios of MEF cells. Heatmap of the nucleotide ratios is shown in left and the ratio values are shown in right (n = 3). (B) The effect of metformin on energy states of MEF cells. The cellular energy state was calculated by formula (ATP + 0.5 × ADP) / (ATP + ADP + AMP) [31] (n = 3). (C) The effect of metformin on NAD^{+}/NADH ratio of MEF cells (n = 3). Data are expressed as mean ± SD. $^{*}p < 0.05$, $^{**}p < 0.01$ and $^{***}p < 0.001$ vs. the control group.

independently accumulated following metformin treatment, whereas the proportions of fumarate (M + 2), malate (M + 2), α-KG (M + 2), citrate (M + 4), malate (M + 4), α-KG (M + 4), succinate (M + 4) and citrate (M + 6) were significantly decreased in an Ampkα-independent manner. These results indicated that metabolic flux from acetyl-CoA to TCA cycle through citrate synthase was Ampkα-independently repressed. Moreover, the proportions of citrate (M + 3), fumarate (M + 3), malate (M + 3), succinate (M + 3) and α-KG (M + 3) were also Ampkα-independently decreased by metformin treatment, suggesting that pyruvate-malate metabolic flux through pyruvate carboxylase was inhibited (Fig. 5).

Furthermore, the levels of amino acid also exhibited significant changes following metformin treatment. The proportion of aspartate (M + 0) was increased and the proportions of aspartate (M + 2, M + 3, M + 4) were all decreased in both WT and KO MEF cells, suggesting that malate-aspartate shuttle was inhibited following metformin treatment (Fig. 5). Similarly, the proportion of glutamate (M + 0) was increased and the proportions of glutamate (M + 3, M + 4, M + 5) were all decreased in both WT and KO MEF cells (Fig. 5). These findings indicated that the amino acids generated from TCA cycle were also Ampkα-independently inhibited by metformin.

3.5. Metformin-Mediated Ampkα-independent Metabolic Reprogramming Was Concentration-independent

It has been reported that treatment with low or high concentration of metformin can result in different effects on cells [36]. In order to further examine whether AMPKα independence of metformin-induced metabolic alterations correlates with its concentration, we investigated the impact of different concentrations of metformin (1 and 10 mM) on cell proliferation and metabolic alterations in WT and KO MEF cells. Of note, metformin concentration-dependently induced phosphorylation of Ampkα and suppressed the proliferation of WT MEF cells, but also exerted a similar anti-proliferative effect on KO MEF cells (Fig. 6A–B). We have also determined the levels of Acc1, P-Acc, S6, P-S6, mTor, P-mTor, Lc3, Atgl, Erk and P-Erk in MEF cells following low and high-concentration of metformin treatment. As shown in Fig. 6A, 1 mM metformin displayed a slight promotion on P-Ampk and P-Acc as well as a slight inhibition on P-Erk and Lc3 compared to 10 mM metformin.

Furthermore, GC–MS metabolomics profiling showed that metformin also affected metabolic pathways of MEF cells in a concentration-dependent manner, as evidenced by fewer differential metabolites found in MEF cells

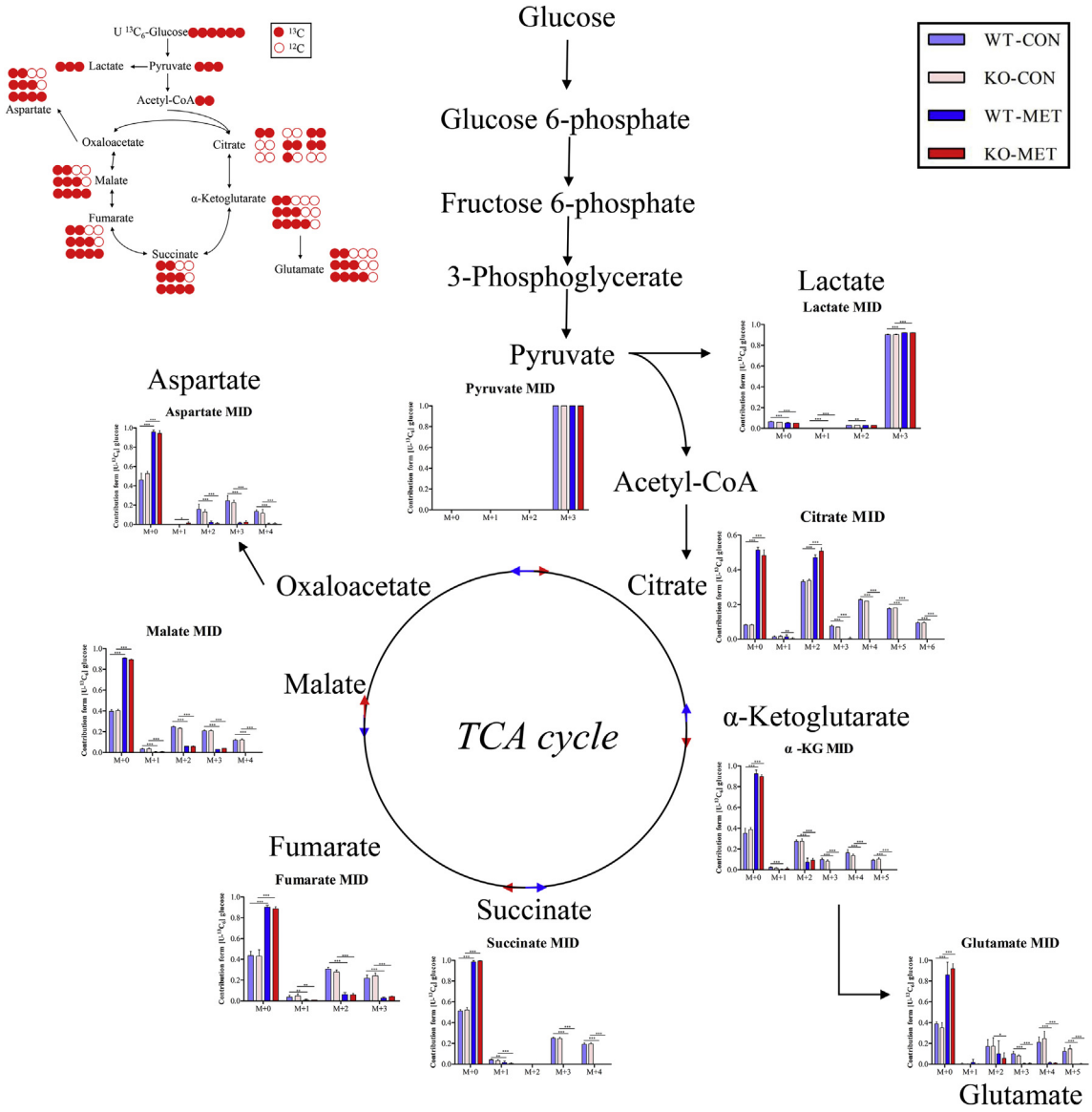

Fig. 5. Metabolic flux analysis of metformin induced metabolic changes by using U-$^{13}C_6$-glucose as tracer. (n = 5. CON indicates control, MET indicates metformin and MID indicates mass isotopologue distribution. Data are expressed as mean ± SD. $^{*}p < 0.05$, $^{**}p < 0.01$ and $^{***}p < 0.001$ vs. the control group.)

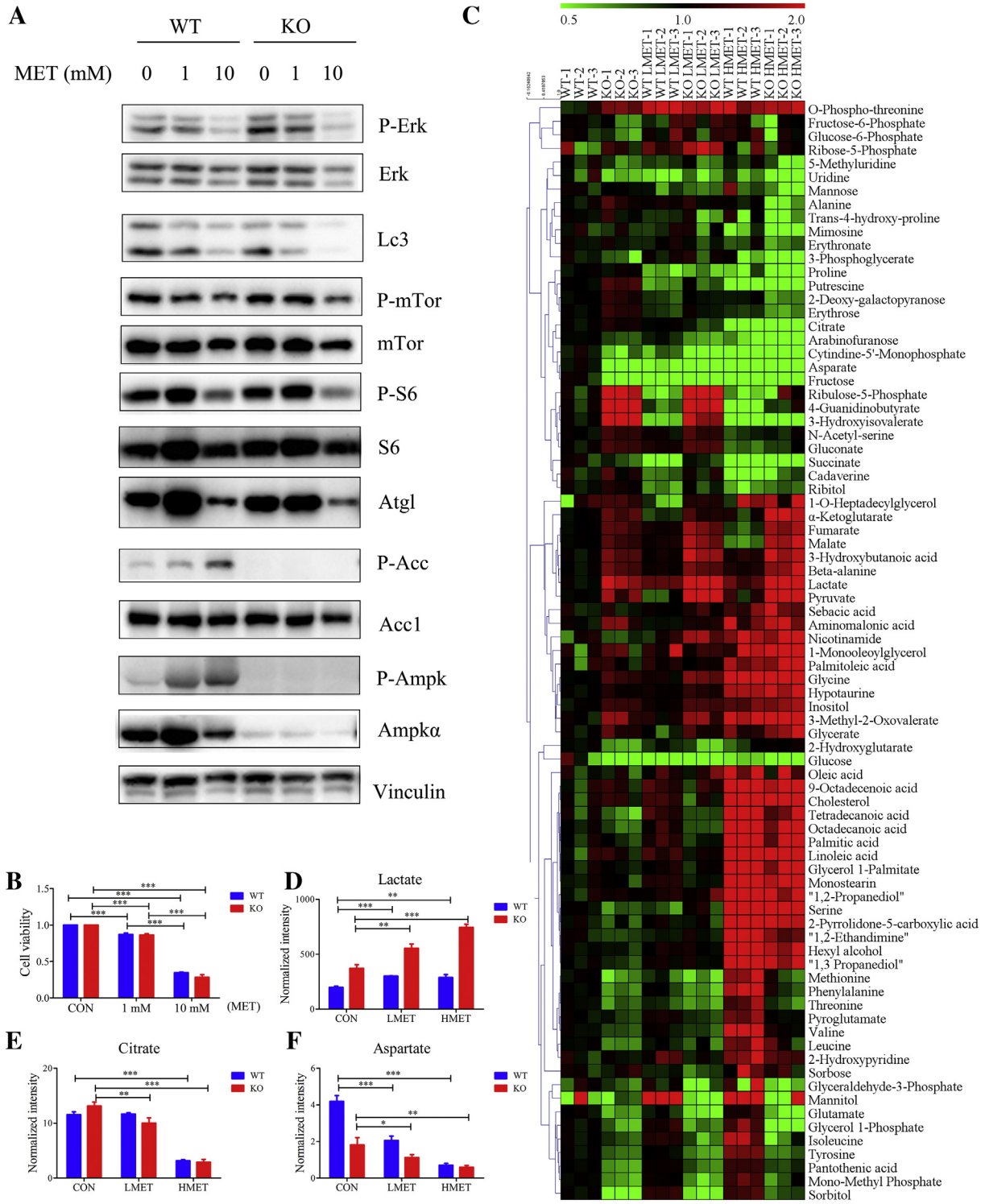

Fig. 6. Low concentration of metformin affected cellular metabolism in an Ampkα-independent manner. (A) The effects of metformin with low and high concentrations (1 mM and 10 mM) on Ampkα, P-Ampk, Acc1, P-Acc (S79), S6, P-S6 (S235/236), mTor, P-mTor (S2448), Lc3, Atgl, Erk and P-Erk (Thr202/Tyr204) in MEF cells after 24 h of treatment. Vinculin was used as a loading control. (B) The effects of metformin with low and high concentrations (1 mM and 10 mM) on cell viability following 48 h of treatment. (n = 4) (C) Heatmap of main metabolites in WT and KO MEF cells following 24 h of treatments with metformin (1 mM and 10 mM) based on GC–MS (n = 3). (D–F) The levels of lactate, citrate and aspartate in MEF cells treated with different concentrations of metformin (1 mM and 10 mM) were compared (n = 3). Data are expressed as mean ± SD. $^{*}p < 0.05$, $^{**}p < 0.01$ and $^{***}p < 0.001$ vs. the control group. LMET indicates a low concentration of metformin (1 mM), and HMET indicates a high concentration of metformin (10 mM).

treated with 1 mM metformin compared to 10 mM metformin (Fig. 6C). Similar to high concentration of metformin, the levels of lactate in both WT and KO MEF cells were also elevated following treatment with 1 mM metformin (Fig. 6D). However, 1 mM metformin had little effect on the TCA cycle (Fig. 6E). In line with the previous observations [37], the level of aspartate was markedly reduced by both treatments with metformin (Fig. 6F). These results suggest that metformin-mediated Ampkα-independent metabolic reprogramming did not depend on its concentrations.

3.6. Energy Stress by FBS Starvation Also Led to Ampkα-independent Alterations in Metabolic Pathways

FBS starvation is considered as a common model for energy stress, which can activate AMPK phosphorylation. Thus, the metabolomics profiling of WT and KO MEF cells under FBS-free condition was analyzed to further confirm the correlation between metabolic reprogramming and Ampkα activity. As expected, FBS starvation induced obvious phosphorylation of Ampkα in WT MEF cells but not in KO MEF cells (Fig. S6A). Consistently, the intracellular glucose was Ampkα-independently increased and the levels of lactate and citrate were Ampkα-independently reduced by FBS-free culture (Fig. S6D). Next, we also compared the metabolic alterations between WT and KO MEF cells under FBS-free condition. As Fig. S6B and C shown, the two most markedly differential metabolic pathways were alanine, aspartate and glutamate metabolism as well as TCA cycle, which was in line with the metabolic differences between two MEF cell lines cultured with FBS. These results indicated that FBS starvation could also induce metabolic reprogramming bypassing Ampkα.

3.7. Metformin AMPKα-independently Induced Metabolic Alterations and Inhibited Tumorigenicity in Human Cell Lines

To further confirm the AMPKα independence of metformin on cellular metabolism, we used MCF10A shControl and shPRKAA1 cells to validate the AMPKα independence of metformin (Fig. 7A). After *PRKAA1* knocking down, decreased levels of P-AMPK and P-ACC as well as increased level of P-S6 were observed (Fig. 7A). Following metformin treatment, lactate to pyruvate ratio and various amino acids were increased, while citrate and aspartate were decreased in both MCF10A shControl and shPRKAA1 cells (Fig. 7B), in line with the observations in MEF lines.

Also, we conducted GC–MS metabolomics to examine the effect of metformin on hepatic cell lines with different levels of AMPKα expression. Based on the AMPKα levels in ten of hepatic cell lines (Fig. 8A), HCCLM3 and BEL-7402 were chosen as AMPK high-expressing cells, while SMMC-7721 was used as AMPK low-expressing cells. Interestingly, these three cell lines exhibited similar sensitivity in response to treatment with 10 mM metformin (Fig. 8B). Consistent with the effects observed in MEF and MCF10A cells, metformin dramatically promoted the lactate production from pyruvate and suppressed the TCA cycle in three HCC cell lines (Fig. 8C). Moreover, following metformin treatment, numerous amino acids of three cell lines were altered in a consistent way. Therefore, these findings suggest that the effects of metformin on cellular metabolism may be largely bypassing AMPKα.

Finally, to test whether the effect of metformin on tumorigenicity is dependent on AMPKα, we performed colony formation assays by using AMPKα high-expressing MHCC97H and BEL-7402 cells as well as AMPKα low-expressing SMMC-7721 and SNU-449 cells. The results showed that metformin obviously inhibited colony formation in both AMPKα high-expressing and low-expressing HCC cell lines based on both two and three-dimensional colony formation assays (Fig. 8D, Fig. S7). Of note, we knocked down *PRKAA1* in MHCC97H cells and also found that metformin remarkably suppressed clonogenicity in both MHCC97H shControl and shPRKAA1 cells (Fig. S8). Taken together, these findings indicated that metformin could AMPKα-independently inhibited tumorigenicity in HCC cell lines.

4. Discussion

As a first-line anti-hyperglycemic drug and a potential anti-cancer agent, metformin has gained considerable attention to its mechanisms of action. It has been well accepted that metformin functions through disturbing the metabolic processes [8,9,37,38]. Moreover, AMPK has been reported to serve as a critical modulator for the action of metformin [39]. However, it is still unclear whether metformin-mediated metabolism disturbance attributes to AMPK activation. Hence, the overall aim of this study was to investigate the AMPKα dependence of effect of metformin on metabolism. Here, we comprehensively evaluated the effect of metformin on metabolism in *Prkaa1* WT and KO MEF cells based on GC–MS and CE–MS metabolomics analyses as well as metabolic flux analysis. As expected, metformin treatment resulted in significant alterations to metabolic pathways, including the TCA cycle, glycolysis, amino acid metabolism and nucleoside levels. Importantly, most of these changes induced by metformin did not depend on Ampkα except for some individual metabolites, which was consistent with the observations in MEF cells with AICAR treatment or under FBS-free condition as well as in metformin-treated HCC and MCF10A cells.

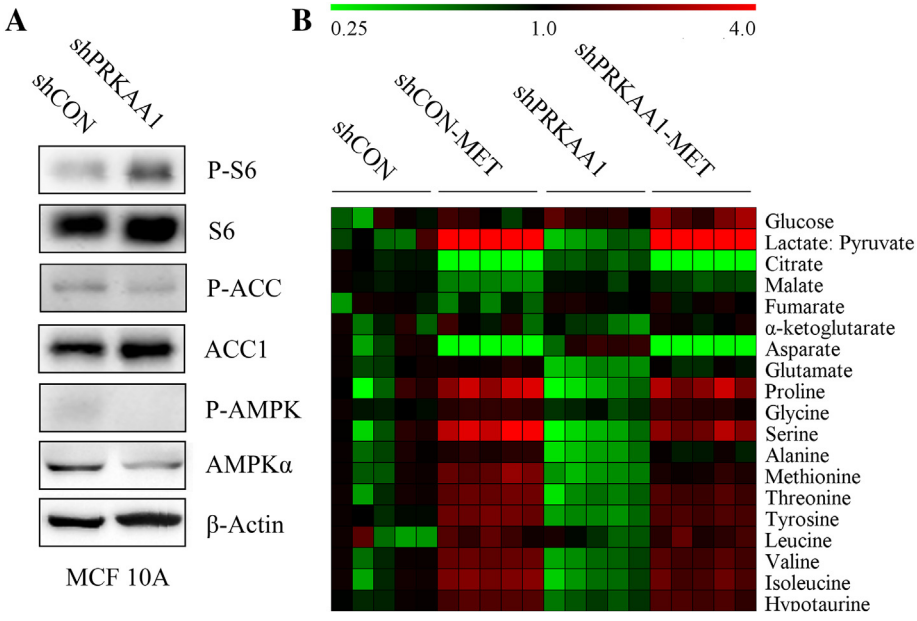

Fig. 7. The effects of metformin on metabolism of MCF10A cells did not depend on AMPKα. (A) Immunoblot of AMPKα, P-AMPK (T172), ACC1, P-ACC (S79), S6 and P-S6 (S235/236) in MCF10A shControl and shPRKAA1 cells. β-Actin was used as internal control. (B) Heatmap of main metabolites altered by metformin after treatment for 24 h (20 mM, n = 5). For each metabolite, the average value of untreated shControl group was used for normalization.

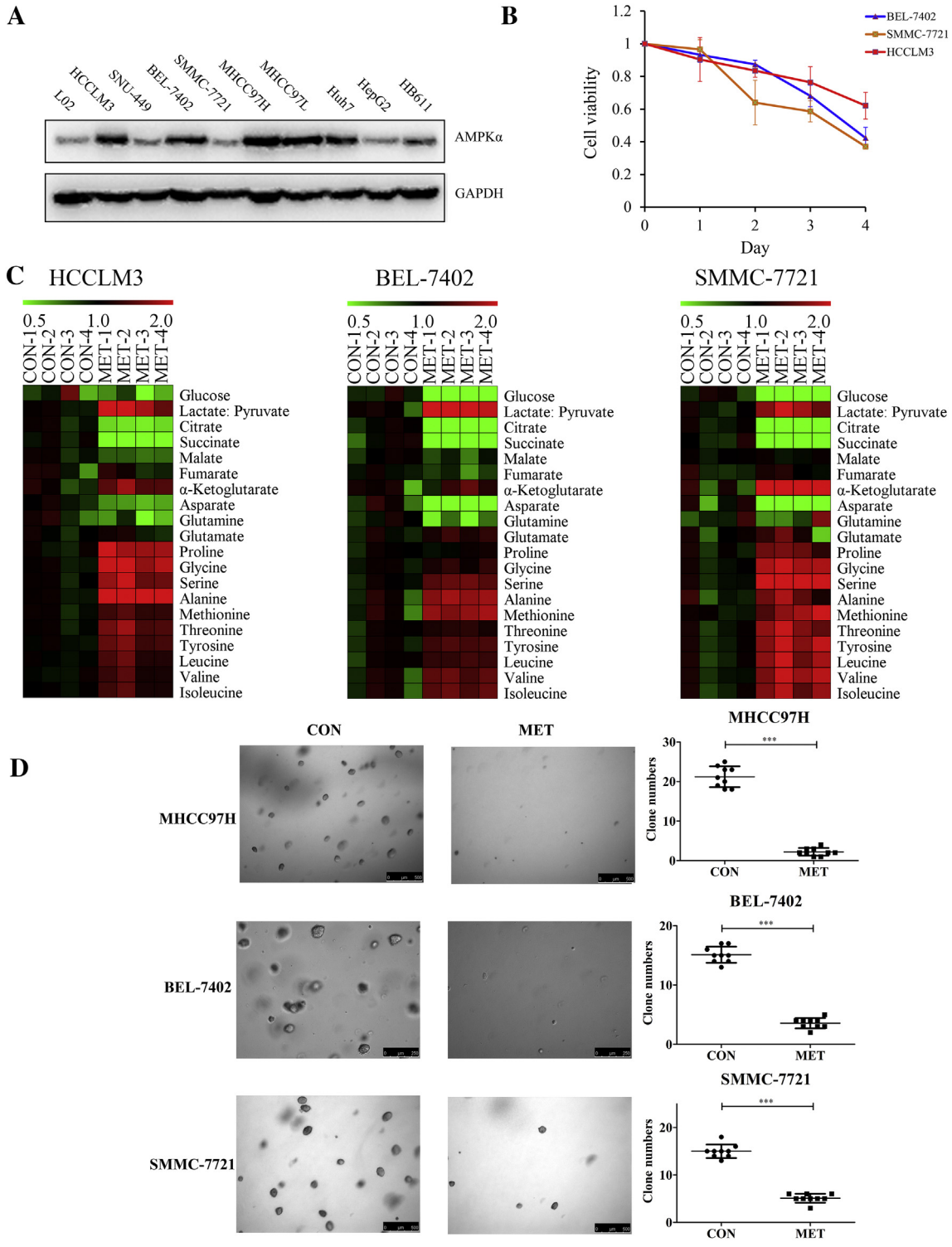

Fig. 8. The effects of metformin on metabolism and clonogenicity of human hepatocellular carcinoma (HCC) cells did not depend on AMPKα. (A) Immunoblot of AMPKα in ten of hepatic cell lines. GAPDH was used as an internal control. (B) The effect of metformin (10 mM) on cell viability of HCCLM3, BEL-7402 and SMMC-7721 cells (n = 3). (C) Heatmap of main metabolites altered by metformin treatment for 24 h in HCCLM3, BEL-7402 and SMMC-7721 cells (n = 4). (D) Three-dimensional colony formation assay by 10 mM metformin treatment in MHCC97H, BEL-7402 and SMMC-7721 cells (n = 9. Data are expressed as mean ± SD. $^{***}p < 0.001$ vs. the control group.)

Increasing evidence shows that metformin exhibited anticancer and hypoglycemic effects in an AMPK-independent way, although AMPK signaling pathway could be triggered by metformin [20,21]. Of note, our study also demonstrated that metformin affected cellular metabolism largely bypassing Ampkα. We observed an Ampkα-independent elevation in lactate/pyruvate ratio and reduction in citrate/pyruvate ratio following metformin treatment, suggesting that pyruvate was more inclined to enter into lactate than the TCA cycle. Importantly, these metabolic alterations were also validated by metabolic flux analysis (Fig. 5). Additionally, we found that metformin led to a marked decrease in NAD^+/NADH ratio, which can be partly explained that the NADH generated from glycolysis could not be converted into NAD^+ via the oxidative phosphorylation. These results could be supported by the previous reports that metformin could inhibit mitochondrial

complex I in respiratory chain [40] as well as reduced hepatic energy state AMPK-independently [21]. Furthermore, AMPK has been considered as a suppressor of tumorigenesis [41]. Interestingly, we observed that *Prkaa1* WT and KO MEF cells exhibited similar growth rates with or without metformin treatment. Moreover, glutamine and sodium pyruvate could reverse metformin-induced growth inhibition regardless of Ampkα. Consistent with our results, metformin has been reported to elevate the dependence of glutamine metabolism in prostate cancer cells [42]. We also found that metformin could Ampkα-dependently upregulated P-Acc but Ampkα-independently downregulated the levels of P-mTor, P-S6, P-Erk, Atgl and Lc3. These results suggested metformin might lead to an Ampkα-dependent inhibition in fatty acid synthesis while an Ampkα-independent suppression in protein synthesis, autophagy and fatty acid catabolism in MEF cells, which were consistent with previous findings [36,43,44].

Here, our studies mainly revealed an Ampkα-independence of metformin-mediated metabolic alterations, which could provide several clinical significances. Although increasing clinical studies have showed that metformin could reduce incidence and mortality of cancer [4,45], the effects of metformin vary among different populations [46,47]. Besides, the acquired drug-resistance also occurred during metformin treatment for cancer [48]. According to metabolic pathway analyses, the drug-resistance of metformin might be due to the activation of complementary metabolic pathway to TCA cycle, which was independent of the activity of AMPKα. Hence, these findings suggest that the other activators of AMPKα may also not work during the drug-resistance of metformin. Moreover, these also provide a new insight that combination of metformin with the inhibitors of complementary metabolic pathway to TCA cycle may achieve better therapeutic benefits.

AICAR, as a direct AMPK agonist, has also been reported to possess hypoglycemic and antitumor effects [49,50]. Several previous studies showed that the antitumor effects of AICAR correlated with AMPK activity [51,52]. However, some recent reports have revealed that such effects can be mediated by AMPK-independent mechanisms [53,54]. Previous studies showed that AICAR could lead to pyrimidine starvation and apoptosis in multiple myeloma cells [35] as well as inhibit glycolysis in human umbilical vein endothelial cells [55]. Consistently, we observed a dramatic upregulation in purine metabolism and downregulation in pyrimidine metabolism as well as lactate/pyruvate ratio in AICAR-treated MEF cells. Moreover, in addition to nucleotide metabolism and glycolysis, AICAR also suppressed the TCA cycle in MEF cells, suggesting an energy stress by AICAR. Here, our data indicated that metformin and AICAR displayed opposite effects on glycolysis, despite the fact that Ampkα was activated by both treatments. It was more surprising that these observed metabolism alternations stimulated by metformin and AICAR were largely Ampkα-independent. Recently, AMPK has been reported to play a key role in FBS starvation-induced increase of glucose transport [56]. However, similar to AICAR, FBS-starvation also resulted in a decrease in lactate and citrate bypassing Ampkα. Furthermore, metformin-mediated AMPKα-independent metabolism reprogramming also be validated in human HCC cell lines with distinct AMPKα expressions as well as in MCF10A shControl and shPRKAA1 cells. Taken together, these results suggest that metformin could AMPKα-independently alter cellular metabolism in different origin cells.

On the other hand, several previous studies revealed that metformin acted as an antitumor agent in multiple cancers via activating AMPK [19,57]. Additionally, a recent report showed that at the initial stage of administration in rat models of diabetes, metformin could lower hepatic glucose production in a duodenal Ampk-dependent mode [18]. Consistently, we observed that several amino acids including phenylalanine, methionine and threonine were affected by metformin related to Ampkα activation. Moreover, the metformin induced nucleotide changes were partly Ampkα-dependent. Specifically, it has been reported that AMPK dependence of metformin might be associated with its concentrations [36]. That study showed that low-concentration of metformin (≤1 mM) Ampk-dependently suppressed mTorc1 signaling pathways in primary hepatocytes, whereas high-concentration of metformin (>2 mM) exhibited an Ampk-independent mTorc1 inhibition. However, our data indicated that 1 mM metformin also affected metabolism of MEF cells bypassing Ampkα, even though the metabolic pathways displayed slighter alterations following 1 mM metformin treatment compared to 10 mM. Nevertheless, despite these findings, one limitation of the present study was only at cellular level. Thus, further research will be needed to illuminate the exact mechanisms of AMPKα dependence of metformin in vitro and in vivo as well as in humans.

In summary, based on multi-platform metabolomics analyses and metabolic flux analysis, we found that metformin displayed strong influence on metabolic pathways in *Prkaa1* WT and KO MEF cells. Specifically, metformin treatment led to an elevation in glycolysis, a reduction in the TCA cycle and energy states, as well as a disturbance in amino acid metabolism. Importantly, metformin-mediated metabolism programming was largely independent of Ampkα, with the exception of several amino acids and nucleotides. Consistently, such Ampkα independence of metformin was validated in HCC cell lines with distinct AMPKα expressions as well as in MCF10A shControl and shPRKAA1 cells. Moreover, we demonstrated that AICAR Ampkα-independently inhibited glycolysis and TCA cycle as well as disrupted nucleotide metabolism. Our results highlight a systematic view of metabolomics profiling mediated by metformin and AICAR as well as the Ampkα independence, providing a new insight for their application.

Acknowledgements

This study is supported by the National Key Research and Development Program of China (2016YFC0903302), National Natural Science Foundation of China grants (No. 81672440), Innovation program of science and research from the DICP, CAS (DICP TMSR201601) and the 100 Talents Program of Chinese Academy of Sciences.

Author Contributions

M.Y., H.Q., G.X. and H.-L.P. designed the research, M.Y. did the experiment, M.Y., H.Q., T.X., X.Z., W.W., H.C., X.L., J.L., D.C., X.L., G.X. and H.-L. P. analyzed data, M.Y., H.Q., G.X. and H.-L.P. wrote the manuscript.

Conflict of Interest

The authors declare no competing financial interests.

Appendix A. Supplementary data

Supplementary data to this article can be found online at https://doi.org/10.1016/j.metabol.2018.11.010.

References

[1] Viollet B, Guigas B, Sanz Garcia N, Leclerc J, Foretz M, Andreelli F. Cellular and molecular mechanisms of metformin: an overview. Clin Sci 2012;122:253–70.
[2] Zakikhani M, Dowling R, Fantus IG, Sonenberg N, Pollak M. Metformin is an AMP kinase-dependent growth inhibitor for breast cancer cells. Cancer Res 2006;66:10269–73.
[3] Hirsch HA, Iliopoulos D, Tsichlis PN, Struhl K. Metformin selectively targets cancer stem cells, and acts together with chemotherapy to block tumor growth and prolong remission. Cancer Res 2009;69:7507–11.
[4] Evans JMM, Donnelly LA, Emslie-Smith AM, Alessi DR, Morris AD. Metformin and reduced risk of cancer in diabetic patients. Br Med J 2005;330:1304–5.
[5] Anisimov VN, Berstein LM, Egormin PA, Piskunova TS, Popovich IG, Zabezhinski MA, et al. Metformin slows down aging and extends life span of female SHR mice. Cell Cycle 2008;7:2769–73.
[6] Barzilai N, Crandall JP, Kritchevsky SB, Espeland MA. Metformin as a tool to target aging. Cell Metab 2016;23:1060–5.
[7] Wu H, Esteve E, Tremaroli V, Khan MT, Caesar R, Manneras-Holm L, et al. Metformin alters the gut microbiome of individuals with treatment-naive type 2 diabetes, contributing to the therapeutic effects of the drug. Nat Med 2017;23:850–61.

[8] Liu X, Romero IL, Litchfield LM, Lengyel E, Locasale JW. Metformin targets central carbon metabolism and reveals mitochondrial requirements in human cancers. Cell Metab 2016;24:728–39.
[9] Griss T, Vincent EE, Egnatchik R, Chen J, Ma EH, Faubert B, et al. Metformin antagonizes cancer cell proliferation by suppressing mitochondrial-dependent biosynthesis. PLoS Biol 2015;13:e1002309.
[10] Gwinn DM, Shackelford DB, Egan DF, Mihaylova MM, Mery A, Vasquez DS, et al. AMPK phosphorylation of raptor mediates a metabolic checkpoint. Mol Cell 2008;30:214–26.
[11] Canto C, Gerhart-Hines Z, Feige JN, Lagouge M, Noriega L, Milne JC, et al. AMPK regulates energy expenditure by modulating NAD(+) metabolism and SIRT1 activity. Nature 2009;458:1056–U140.
[12] Shi WY, Xiao D, Wang L, Dong LH, Yan ZX, Shen ZX, et al. Therapeutic metformin/AMPK activation blocked lymphoma cell growth via inhibition of mTOR pathway and induction of autophagy. Cell Death Dis 2012;3:e275.
[13] Kim J, Kundu M, Viollet B, Guan K-L. AMPK and mTOR regulate autophagy through direct phosphorylation of Ulk1. Nat Cell Biol 2011;13:132–U71.
[14] Eid AA, Ford BM, Block K, Kasinath BS, Gorin Y, Ghosh-Choudhury G, et al. AMP-activated protein kinase (AMPK) negatively regulates Nox4-dependent activation of p53 and epithelial cell apoptosis in diabetes. J Biol Chem 2010;285:37503–12.
[15] Hardie DG. AMP-activated/SNF1 protein kinases: conserved guardians of cellular energy. Nat Rev Mol Cell Biol 2007;8:774–85.
[16] Zhang BB, Zhou G, Li C. AMPK: an emerging drug target for diabetes and the metabolic syndrome. Cell Metab 2009;9:407–16.
[17] Hardie DG. AMPK: a target for drugs and natural products with effects on both diabetes and cancer. Diabetes 2013;62:2164–72.
[18] Duca FA, Cote CD, Rasmussen BA, Zadeh-Tahmasebi M, Rutter GA, Filippi BM, et al. Metformin activates a duodenal Ampk-dependent pathway to lower hepatic glucose production in rats. Nat Med 2015;21:506–11.
[19] Storozhuk Y, Hopmans SN, Sanli T, Barron C, Tsiani E, Cutz JC, et al. Metformin inhibits growth and enhances radiation response of non-small cell lung cancer (NSCLC) through ATM and AMPK. Br J Cancer 2013;108:2021–32.
[20] Ben Sahra I, Regazzetti C, Robert G, Laurent K, Le Marchand-Brustel Y, Auberger P, et al. Metformin, independent of AMPK, induces mTOR inhibition and cell-cycle arrest through REDD1. Cancer Res 2011;71:4366–72.
[21] Foretz M, Hebrard S, Leclerc J, Zarrinpashneh E, Soty M, Mithieux G, et al. Metformin inhibits hepatic gluconeogenesis in mice independently of the LKB1/AMPK pathway via a decrease in hepatic energy state. J Clin Investig 2010;120:2355–69.
[22] Zhang C-S, Jiang B, Li M, Zhu M, Peng Y, Zhang Y-L, et al. The lysosomal v-ATPase-ragulator complex is a common activator for AMPK and mTORC1, acting as a switch between catabolism and anabolism. Cell Metab 2014;20:526–40.
[23] Zhang Y-L, Guo H, Zhang C-S, Lin S-Y, Yin Z, Peng Y, et al. AMP as a low-energy charge signal autonomously initiates assembly of AXIN-AMPK-LKB1 complex for AMPK activation. Cell Metab 2013;18:546–55.
[24] Yi Y, Chen D, Ao J, Sun S, Wu M, Li X, et al. Metformin promotes AMP-activated protein kinase-independent suppression of ΔNp63α protein expression and inhibits cancer cell viability. J Biol Chem 2017;292:5253–61.
[25] Ye G, Liu Y, Yin P, Zeng Z, Huang Q, Kong H, et al. Study of induction chemotherapy efficacy in oral squamous cell carcinoma using pseudotargeted metabolomics. J Proteome Res 2014;13:1994–2004.
[26] Zeng J, Yin P, Tan Y, Dong L, Hu C, Huang Q, et al. Metabolomics study of hepatocellular carcinoma: discovery and validation of serum potential biomarkers by using capillary electrophoresis–mass spectrometry. J Proteome Res 2014;13:3420–31.
[27] Xia J, Sinelnikov IV, Han B, Wishart DS. MetaboAnalyst 3.0-making metabolomics more meaningful. Nucleic Acids Res 2015;43:W251–7.
[28] Vincent EE, Coelho PP, Blagih J, Griss T, Viollet B, Jones RG. Differential effects of AMPK agonists on cell growth and metabolism. Oncogene 2015;34:3627–39.
[29] Buzzai M, Jones RG, Amaravadi RK, Lum JJ, DeBerardinis RJ, Zhao F, et al. Systemic treatment with the antidiabetic drug metformin selectively impairs p53-deficient tumor cell growth. Cancer Res 2007;67:6745–52.
[30] Alimova IN, Liu B, Fan Z, Edgerton SM, Dillon T, Lind SE, et al. Metformin inhibits breast cancer cell growth, colony formation and induces cell cycle arrest in vitro. Cell Cycle 2009;8:909–15.
[31] He MX, Gorman MW, Romig GD, Sparks HV. Adenosine formation and myocardial energy status during graded hypoxia. J Mol Cell Cardiol 1992;24:79–89.
[32] Guo D, Hildebrandt IJ, Prins RM, Soto H, Mazzotta MM, Dang J, et al. The AMPK agonist AICAR inhibits the growth of EGFRvIII-expressing glioblastomas by inhibiting lipogenesis. Proc Natl Acad Sci U S A 2009;106:12932–7.
[33] Corton JM, Gillespie JG, Hawley SA, Hardie DG. 5-Aminoimidazole-4-carboxamide ribonucleoside - a specific method for activating AMP-activated protein-kinase in intact-cells. Eur J Biochem 1995;229:558–65.
[34] Harden KK, Robinson JL. Deficiency of UMP synthase in dairy-cattle - a model for hereditary orotic aciduria. J Inherit Metab Dis 1987;10:201–9.
[35] Bardeleben C, Sharma S, Reeve JR, Bassilian S, Frost P, Hoang B, et al. Metabolomics identifies pyrimidine starvation as the mechanism of 5-aminoimidazole-4-carboxamide-1-beta-riboside-induced apoptosis in multiple myeloma cells. Mol Cancer Ther 2013;12:1310–21.
[36] Howell JJ, Hellberg K, Turner M, Talbott G, Kolar MJ, Ross DS, et al. Metformin inhibits hepatic mTORC1 signaling via dose-dependent mechanisms involving AMPK and the TSC complex. Cell Metab 2017;25:463–71.
[37] Gui DY, Sullivan LB, Luengo A, Hosios AM, Bush LN, Gitego N, et al. Environment dictates dependence on mitochondrial complex I for NAD+ and aspartate production and determines cancer cell sensitivity to metformin. Cell Metab 2016;24:716–27.
[38] Pierotti MA, Berrino F, Gariboldi M, Melani C, Mogavero A, Negri T, et al. Targeting metabolism for cancer treatment and prevention: metformin, an old drug with multi-faceted effects. Oncogene 2013;32:1475–87.
[39] Hardie DG, Ross FA, Hawley SA. AMPK: a nutrient and energy sensor that maintains energy homeostasis. Nat Rev Mol Cell Biol 2012;13:251–62.
[40] Owen MR, Doran E, Halestrap AP. Evidence that metformin exerts its anti-diabetic effects through inhibition of complex 1 of the mitochondrial respiratory chain. Biochem J 2000;348:607–14.
[41] Huang X, Wullschleger S, Shpiro N, McGuire VA, Sakamoto K, Woods YL, et al. Important role of the LKB1-AMPK pathway in suppressing tumorigenesis in PTEN-deficient mice. Biochem J 2008;412:211–21.
[42] Fendt S-M, Bell EL, Keibler MA, Davidson SM, Wirth GJ, Fiske B, et al. Metformin decreases glucose oxidation and increases the dependency of prostate cancer cells on reductive glutamine metabolism. Cancer Res 2013;73:4429–38.
[43] Zhou GC, Myers R, Li Y, Chen YL, Shen XL, Fenyk-Melody J, et al. Role of AMP-activated protein kinase in mechanism of metformin action. J Clin Investig 2001;108:1167–74.
[44] Park D-B. Metformin promotes apoptosis but suppresses autophagy in glucose-deprived H4IIE hepatocellular carcinoma cells. Diabetes Metab J 2015;39:518–27.
[45] Gandini S, Puntoni M, Heckman-Stoddard BM, Dunn BK, Ford L, DeCensi A, et al. Metformin and cancer risk and mortality: a systematic review and meta-analysis taking into account biases and confounders. Cancer Prev Res 2014;7:867–85.
[46] Patel T, Hruby G, Badani K, Abate-Shen C, McKiernan JM. Clinical outcomes after radical prostatectomy in diabetic patients treated with metformin. Urology 2010;76:1240–4.
[47] Al Hilli MM, Bakkum-Gamez JN, Mariani A, Cliby WA, Mc Gree ME, Weaver AL, et al. The effect of diabetes and metformin on clinical outcomes is negligible in risk-adjusted endometrial cancer cohorts. Gynecol Oncol 2016;140:270–6.
[48] Scherbakov AM, Sorokin DV, Tatarskiy Jr VV, Prokhorov NS, Semina SE, Berstein LM, et al. The phenomenon of acquired resistance to metformin in breast cancer cells: the interaction of growth pathways and estrogen receptor signaling. IUBMB Life 2016;68:281–92.
[49] Jessen N, Pold R, Buhl ES, Jensen LS, Schmitz O, Lund S. Effects of AICAR and exercise on insulin-stimulated glucose uptake, signaling, and GLUT-4 content in rat muscles. J Appl Physiol 2003;94:1373–9.
[50] Ly P, Kim SB, Kaisani AA, Marian G, Wright WE, Shay JW. Aneuploid human colonic epithelial cells are sensitive to AICAR-induced growth inhibition through EGFR degradation. Oncogene 2013;32:3139–46.
[51] Rattan R, Giri S, Singh AK, Singh I. 5-Aminoimidazole-4-carboxamide-1-beta-D-ribofuranoside inhibits cancer cell proliferation in vitro and in vivo via AMP-activated protein kinase. J Biol Chem 2005;280:39582–93.
[52] Morishita M, Kawamoto T, Hara H, Onishi Y, Ueha T, Minoda M, et al. AICAR induces mitochondrial apoptosis in human osteosarcoma cells through an AMPK-dependent pathway. Int J Oncol 2017;50:23–30.
[53] Guo F, S-Q Liu, Gao X-h, Zhang L-Y. AICAR induces AMPK-independent programmed necrosis in prostate cancer cells. Biochem Biophys Res Commun 2016;474:277–83.
[54] Sid B, Glorieux C, Valenzuela M, Rommelaere G, Najimi M, Dejeans N, et al. AICAR induces Nrf2 activation by an AMPK-independent mechanism in hepatocarcinoma cells. Biochem Pharmacol 2014;91:168–80.
[55] Martinez-Martin N, Blas-Garcia A, Morales JM, Marti-Cabrera M, Monleon D, Apostolova N. Metabolomics of the effect of AMPK activation by AICAR on human umbilical vein endothelial cells. Int J Mol Med 2012;29:88–94.
[56] Ching JK, Rajguru P, Marupudi N, Banerjee S, Fisher JS. A role for AMPK in increased insulin action after serum starvation. Am J Phys Cell Phys 2010;299:C1171–9.
[57] Duan W, Chen K, Jiang Z, Chen X, Sun L, Li J, et al. Desmoplasia suppression by metformin-mediated AMPK activation inhibits pancreatic cancer progression. Cancer Lett 2017;385:225–33.